Agard Conference Proceedings 30,
Hypersonic Boundary Layers and Flow Fields, Ref 12
Royal Aeronautical Society, London, p. 20, 1-3 May 1968.

# EXPERIMENTAL RESULTS FROM THREE CONE-FLOW WAVERIDERS

by

J. Pike

Royal Aircraft Establishment,

Bedford, U.K.

## Summary

Experimental results from three cone flow waveriders.

The 3ft x 4ft high supersonic speed tunnel at R.A.E. Bedford has been used to obtain experimental results from two waverider models with sharp leading edges and a third with a rounded leading edge. At a particular incidence and Mach number (M = 4) the flow supported by the compression surfaces of the models can be predicted theoretically. This predicted flow is shown to agree closely with experimental measurements of lower surface pressures, the shock wave shape and the surface streamline pattern.

At other incidences or Mach numbers the flow cannot be predicted theoretically. The experimental results show however, that for high incidence at M = 4 the pressures are remarkably uniform, and at constant incidence with Mach number decreasing, the shape of the shock wave changes smoothly, including its detachment from the leading edge.

Leading edge rounding is shown to affect pressures only close to the leading edge.

## Introduction

It has been suggested,[1] that lifting configurations may be designed, which at a particular incidence and supersonic Mach number, have a theoretically predictable flow. The design technique involves fitting together compression and expansion surfaces which are the same shape as stream surfaces in known axisymmetric flow fields, to form a 'closed' configuration which has supersonic leading edges, and commonly a bluff base. This design technique is described in more detail in reference 2.

Two models have been constructed whose compression surfaces are the same shape as stream surfaces from the flow about unyawed cones of 11° and 16° semi-angles at M = 4. These models have been tested in the 3ft x 4ft high supersonic speed tunnel at R.A.E. Bedford, to verify that the predicted flow exists, and to investigate the flow at other incidences and Mach numbers.

A third model with a rounded leading edge has also been tested to investigate the effect of leading edge rounding, in case this is necessary for structural reasons.

## 2. Experimental details.

Planforms, sections and pressure hole positions for two of the models are shown at 1/4 scale in figure 1. The compression surfaces are the same shape as stream surfaces in the flow about unyawed circular cones of 11° or 16° semi-vertex angle, in a free stream at M = 4. The surfaces were generated by defining the leading edge in a conical shock wave with vertex 14.35 inches ahead of the nose of the model, and obtaining the surface coordinates by following streamlines in the flow downstream from the leading edge.

All the models were constructed of glass cloth and araldite covering a steel core. Small pressure holes (diameter $\sim$ 0.010 in.) in the compression surface were connected via tubes buried in the glass cloth and araldite to the pressure measuring system pick-up points at the base of the model. The pressures were measured by Midwood manometers[3] with an accuracy of 0.015 in.Hg.

Most of the tests were made with the tunnel at a fixed Mach number of M = 3.977. A variation in Reynolds number from about $10^6$ per foot to about $10^7$ per foot could be obtained by varying the total pressure in the working section from 20 in. Hg to 220 in. Hg. A few tests were made with the variable Mach number facility in operation, giving a Mach number range of 2.5 to 5.

## 3. Comparison of the experimental results with the theoretically predicted flow.

The experimental results are compared with the theoretical flow in three ways, firstly from a comparison of surface pressures along theoretical isobars, secondly from schlieren photographs of the shock wave at various roll angles, and thirdly from oil flow patterns giving the surface streamline pattern.

The position of the pressure holes and theoretical isobars are shown in figure 1. In the isometric view of figure 2, the vertical axis shows pressure coefficients, and the experimental values associated with the pressure holes are compared with theoretical values shown by the 'broken' lines. We see that the experimental pressures closely confirm the theoretical distribution.

Errors in the experimental pressures can come from a number of causes. These can be grouped under five headings, namely errors in model shape, errors in tunnel conditions, deflection of the model in the tunnel, boundary layer effects and errors in the pressure measuring system. The errors in model shape have most significance when measured as errors in model slope. A series of checks showed errors of order 0.002 in/inch as typical, with the model shown in figure 1a having somewhat smaller errors than those of the model shown in figure 1b. The errors in slope could account for up to half the difference between the experimental and theoretical pressure coefficients shown in figure 2. Flow misalignment in the tunnel was allowed for by taking measurements at 0° and 180° of roll. The tunnel incidence measurements were accurate to within 0.05 degree, which is equivalent to about 0.001 in per inch. The test Mach number was 3.977. The reduction of 0.023 in Mach number below the design value would tend to increase the pressures by a small amount. The pressures coefficients have been corrected for sting deflection due to aerodynamic force. Deflection of the glass cloth and araldite near the leading edge of the model due to aerodynamic forces, were eliminated from the model shown in figure 1a by shaping the upper surface to have balancing pressures. The leading edge of the model shown in figure 1b was thick enough to give only small deflections. No correction has been applied for the change in slope due to boundary layer displacement thickness. The boundary layer growth must be expected to increase the pressure slightly near the leading edge. Pressure measuring system inaccuracies could come from pressure holes not perpendicular to the surface, pressure holes which are chipped round the edge, leaks in the pressure tubes or errors in the manometers. The significant effect was found to be the leaks in the pressure tubes, causing a number of pressure holes to be abandoned before the tests

started. This accounts for the gaps in the pressure hole distributions shown in figure 1. The total effect of the errors are such that they could account for the differences in the experimental and theoretical pressure coefficients shown in figure 2.

Figure 3 shows schlieren photographs of the 11° cone flow model at various roll angles. The theoretical shock wave is conical and inclined at 18.5° to the free stream direction. The shock wave shown in figure 3 is straight and in the theoretically predicted position in all three views.

The surface streamlines are illustrated for the 16° cone-flow model in figure 4, by oil flow technique. The line **aa** is the cone axis. As the flow is axisymmetric **aa** is also a theoretical streamline on the surface of the body. The slight deviation of the flow from this line may be accounted for by the boundary layer modifying the direction of the flow near the surface.

The comparisons discussed here, demonstrate clearly, that the theoretically predicted flow does occur in practice.

4. Further experimental results

At conditions other than that for which the compression surface was designed, the flow is not predictable theoretically, and we rely solely on the experimental results for information about the flow.

In figure 5, the pressure distribution for various incidences, with Mach number constant at M = 4, is shown. Zero incidence as shown in figure 5, is the incidence for which the flow is known theoretically. When the surface is inclined to the free stream at less than this incidence, the pressure coefficients are not only small but vary considerably across the surface. For example, in figure 5a we see that at -4° the pressure coefficient has become zero near the wing tips, slightly larger near the nose and reaches a maximum at the centre of the base. This pressure distribution tends to correspond to the local inclination of the compression surface to the free stream. The wing tips of the compression surface are nearly streamwise, the nose in inclined at 3.7° to the free stream and the inclination of the surface increases progressively along the centre line to reach a maximum of 6° at the base.

At positive incidences, the pressure coefficients are remarkably constant across the wing. The characteristic over-compression near the leading edge and resulting expansion in the centre of a flat delta wing with an attached shock wave, does not occur for the shapes tested here. The caret shape near the nose, the smaller incidence of the tips and higher incidence inboard are instrumental in producing the nearly constant pressure.

The ratio of the lift to pressure drag has been obtained by integrating the experimental pressures over the surface. In figure 6 the values obtained are compared with the envelope for plane two-dimensional wedges or caret compression surfaces chosen to be on design at each lift coefficient. The ratio of lift to pressure drag for the cone flow wing is found to be very close to the caret value for a wide range of lift coefficient. For zero lift the pressure drag of any curved surface is finite. Hence the ratio of lift to pressure drag of the cone-flow wing tends to zero as the lift coefficient tends to zero, whereas that of the plane wedge becomes large. The experimental values suggest this divergence at low values of lift coefficient.

With variation of Mach number, the effect of particular interest is the detachment of the shock wave from the leading edge. In figure 3 schlieren photographs of the model and shock wave are shown at various roll angles. From such photographs a series of tangents to the shock wave may be obtained, whose envelope represents the shock wave shape. Shock wave shapes obtained thus at various Mach numbers are shown in figure 7. The main sources of errors in determining the shapes, result from difficulty in exactly locating the edge of the shock wave in some of the photographs, and in constructing the envelope from the finite number of tangents available. However these errors are in general small and give only small changes in the shape, except possibly near the ends of the detached shock waves where the errors may be significant.

At M = 4 the shock wave approximates to an arc of a circle. At higher Mach numbers the shock wave as expected, becomes less convex, and remains firmly attached to the leading edge. As the Mach number decreases below Mach 4, the shock wave detaches smoothly from the leading edge at about M = 3.5 and progressively becomes more remote from the surface.

The rounded leading edge model has a shock wave which is, of course, detached at all Mach numbers. In figure 8, comparison between the sections of the rounded leading edge model and the model derived from the 11° cone-flow are shown. We see that the only difference occurs near the leading edges. The rounded leading edge is semi-circular with 1/4" radius. This radius is large to emphasize the effect of the leading edge rounding. The nose of the rounded leading edge model is part-spherical.

A comparison of the pressures for the two models appears on the left of figure 8. The rounded leading edge has very high pressures on the areas most inclined to the flow, and a rapid

expansion round the leading edge until it meets the compression surface. Recompression to near the original value is complete by about three leading edge diameters inboard or about ten diameters downstream.

Leading edge blunting then makes little difference to the lift coefficient, but the high pressures on forward facing areas will contribute to the drag.

## 5. Conclusions

At the correct conditions of incidence and Mach number, the compression surfaces support the predicted flow to within the limits of experimental error.

Increasing the incidence, whilst keeping the Mach number constant, results in a pressure distribution which is remarkably uniform. The lift to pressure drag ratio is found to be very close to that of a two-dimensional wedge of the same lift coefficient.

The shock wave shape, it is found, becomes increasingly convex with decreasing Mach number, detaching from the leading edge smoothly and becoming remote from the surface at low supersonic Mach numbers.

Leading edge rounding does not affect the pressures on the wing significantly, except over a region of three diameters width from the leading edge, or ten diameters downstream.

References


1. Jones, J.G.
Moore, K.C.
Pike, J.
Roe, P.L.

A method for designing lifting configurations for high supersonic speeds using axisymmetric flow fields.

Ingenieur Archiv
To be published.

2. Seddon, J.
Spence, A.

The use of known flow fields as an approach to the redesign of high speed aircraft.

Agard Conference Proceedings.
Hypersonic Boundary Layers and Flow Fields.
Paper No: 10, May 1968.

3. Anderson, J.R.

Short note on some recent calibrations of R.A.E. automatic self balancing capsule manometers.

Agard Report 163, Note 19, March 1958.

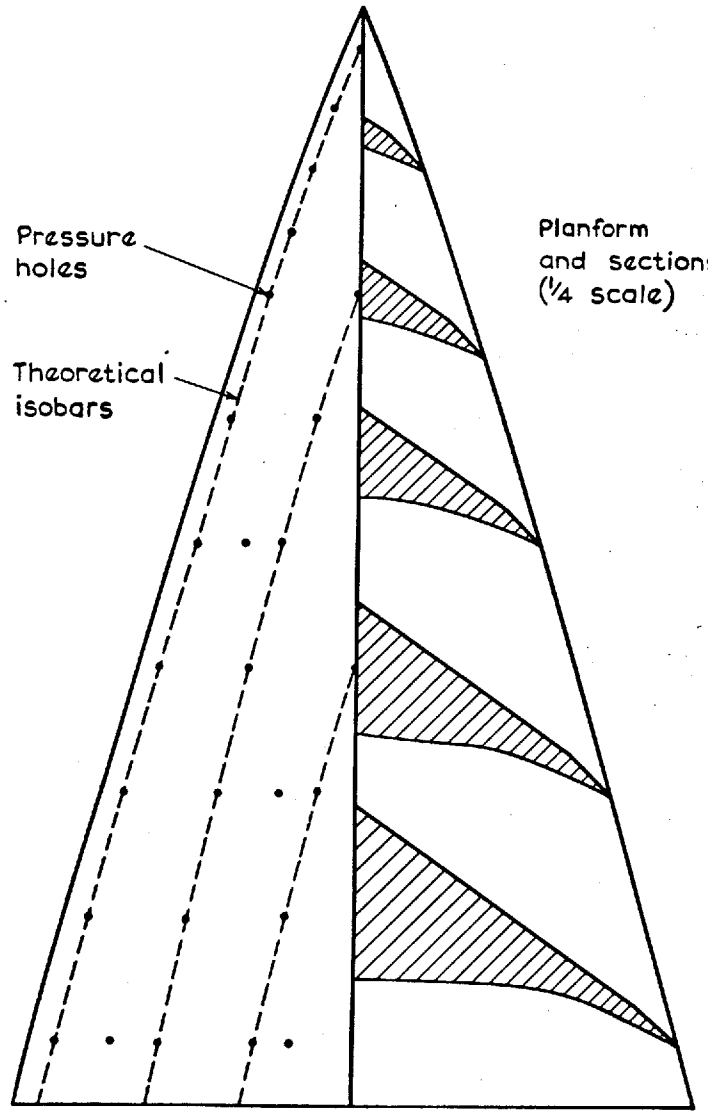


Fig. 1a Planform, sections and pressure hole positions for the model derived from an 11° cone flow

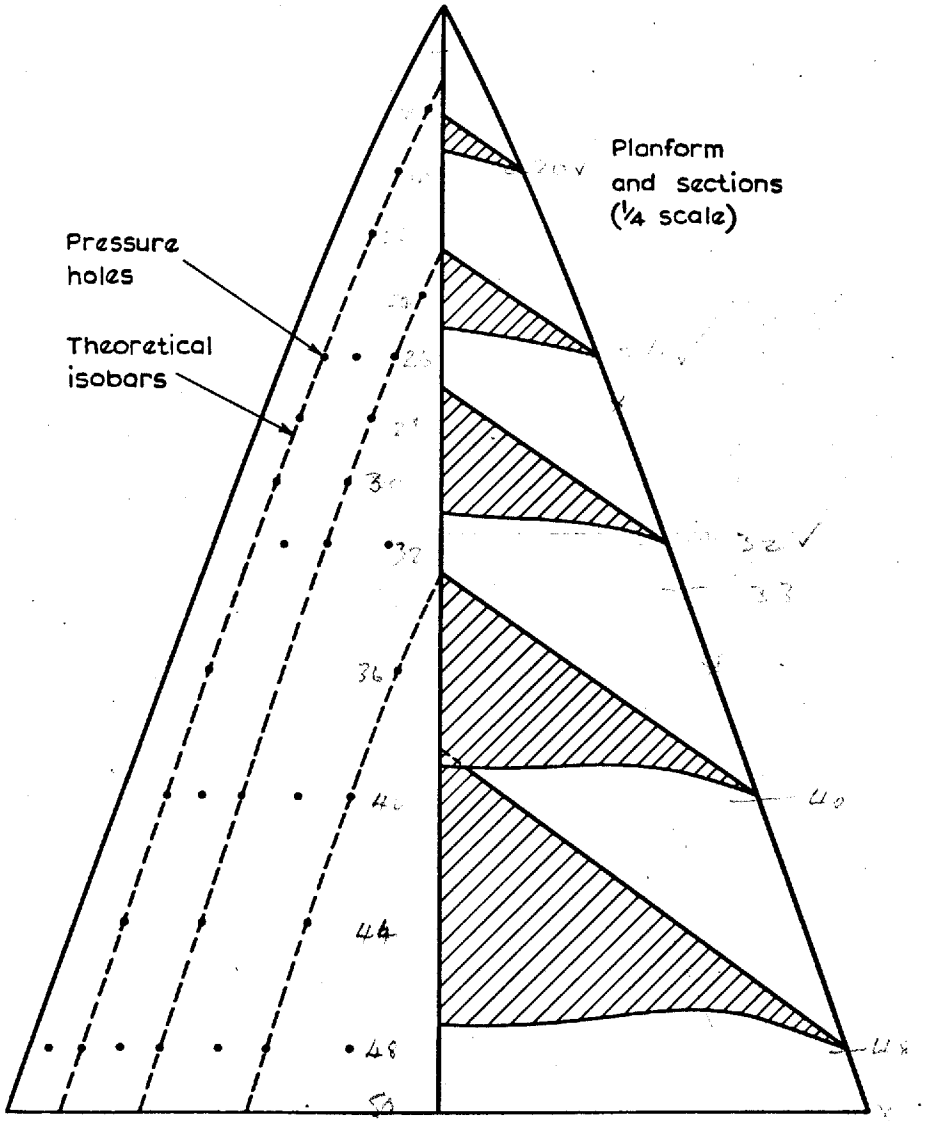


Fig. 1b Planform, sections and pressure hole positions for the model derived from a 16° cone flow

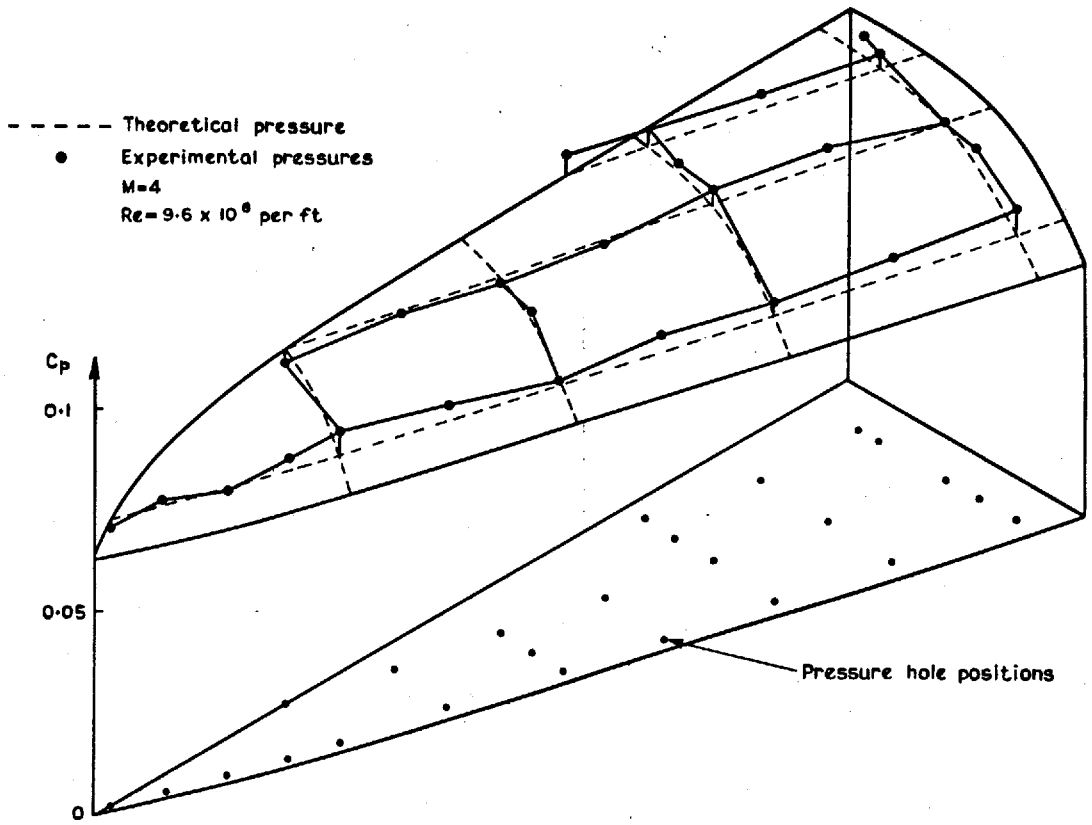


Fig. 2a Comparison of experimental and theoretical pressures (11° cone flow model)

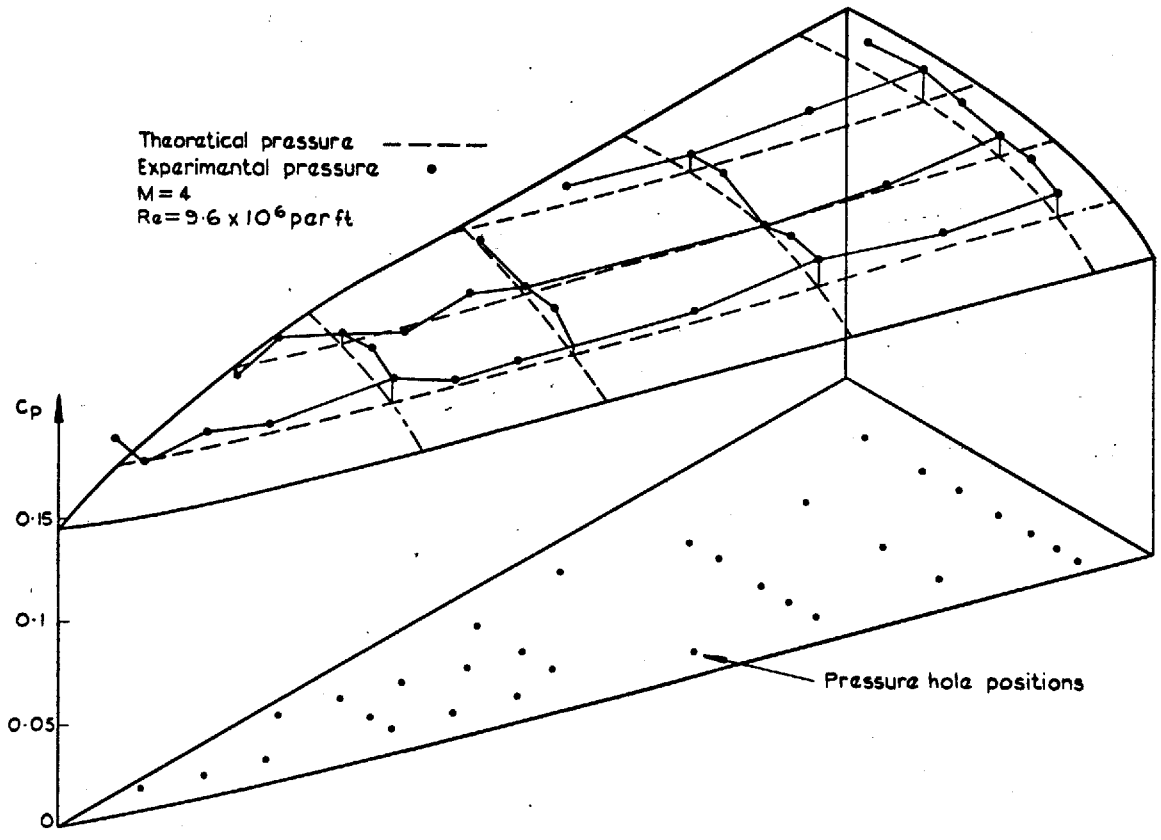


Fig. 2b Comparison of experimental and theoretical pressures (16° cone flow model)

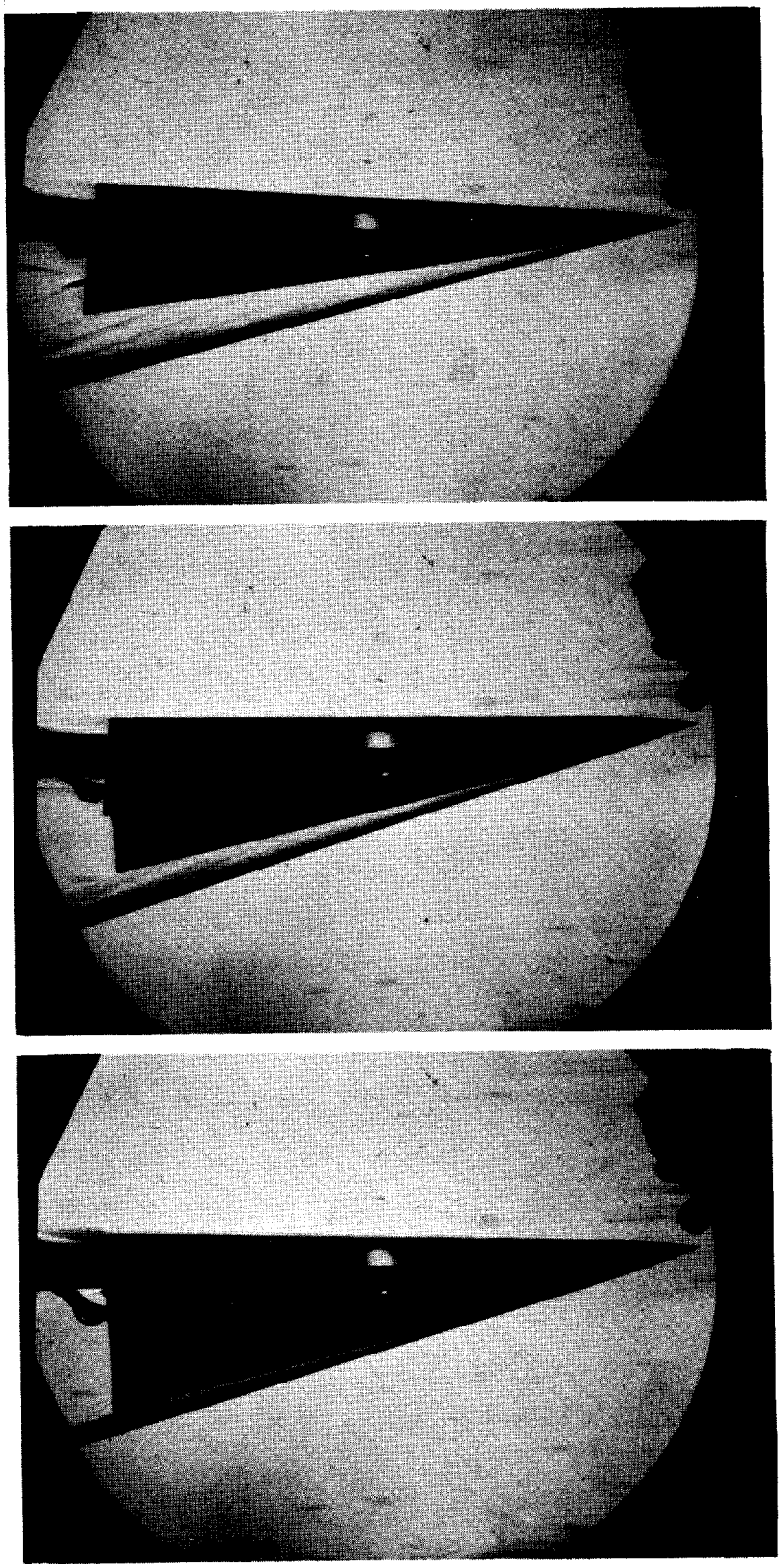

FIG. 3. SCHLIEREN PHOTOGRAPHS OF THE MODEL SUPPORTING A CONICAL SHOCK WAVE, AT M=4 AND AT 0°, 10° AND 20° OF ROLL.

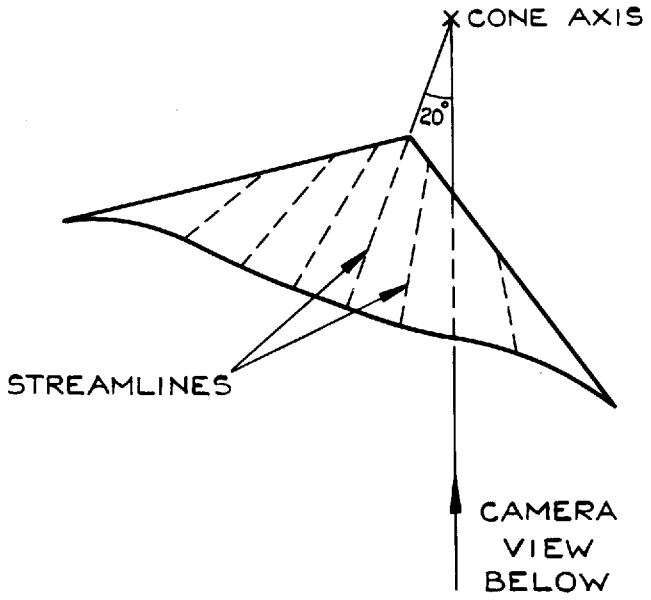


FIG 4A. FRONT VIEW OF MODEL.

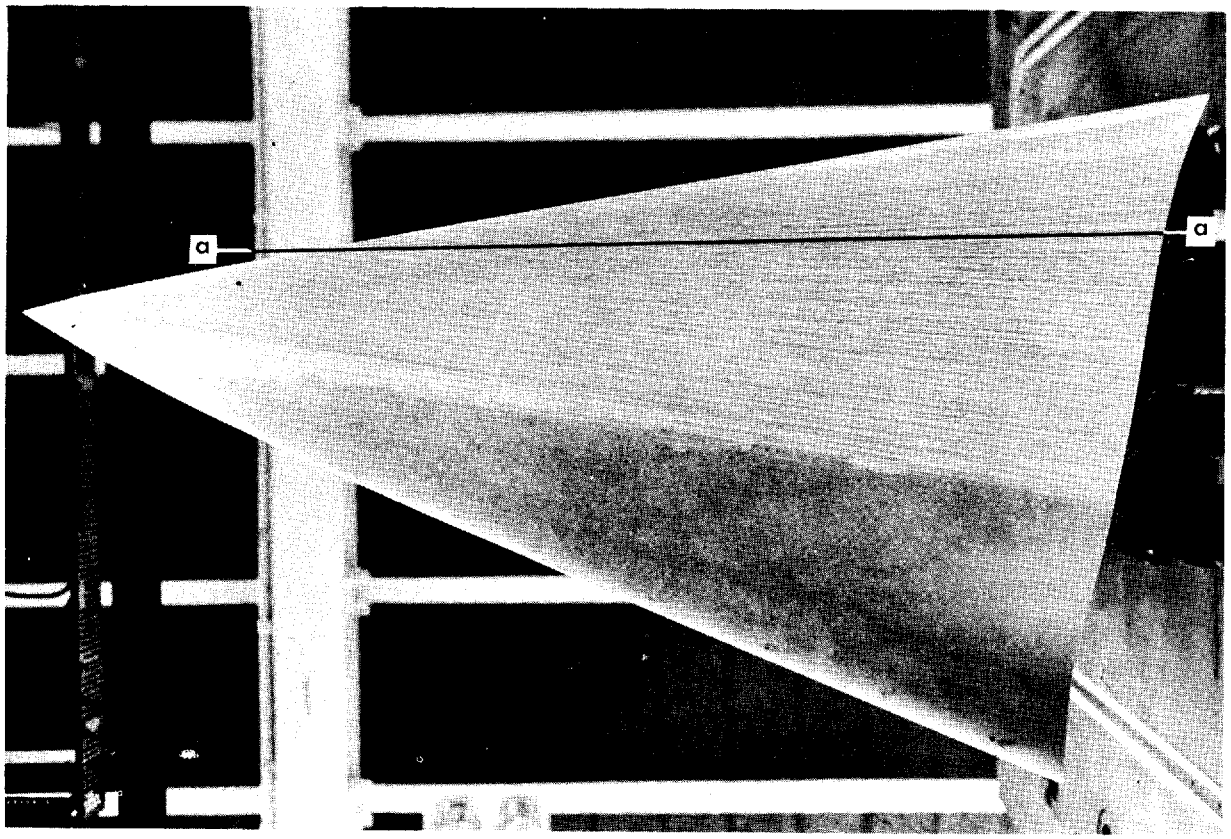


FIG. 4B. OIL FLOW PHOTOGRAPH SHOWING STREAMLINE PATTERN AT M=4 (16° CONE FLOW MODEL).

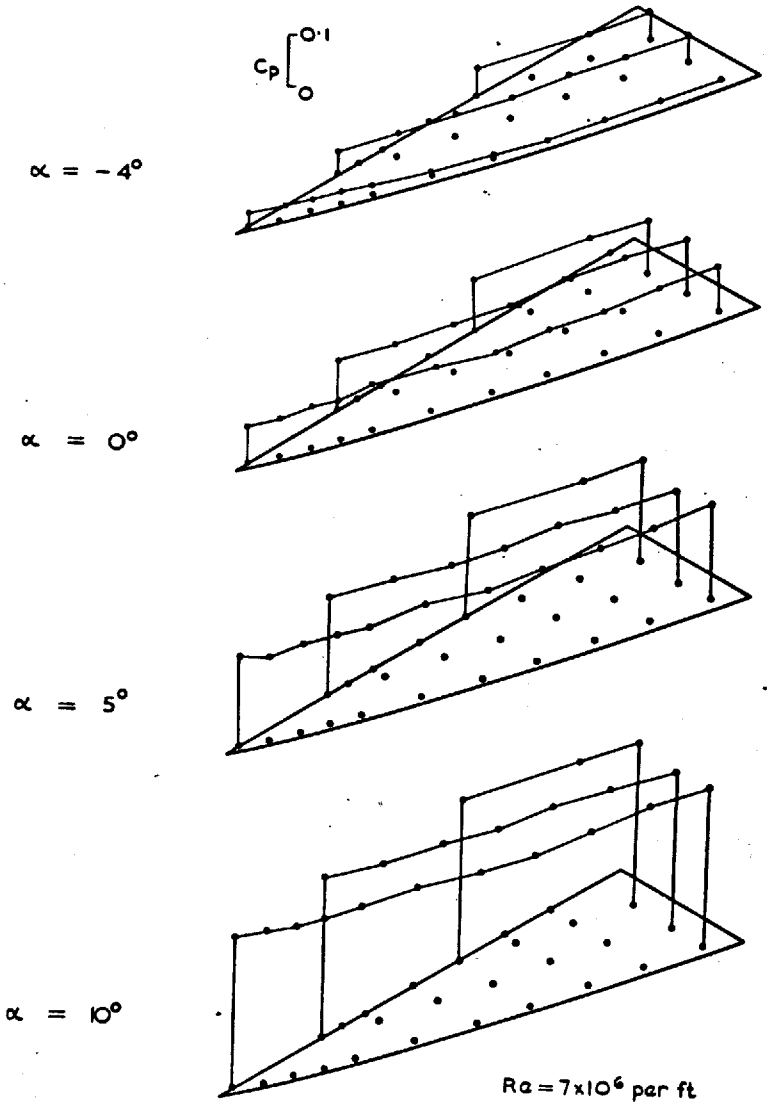


Fig. 5a Experimental pressures on a wing from an 11° cone flow at M = 4

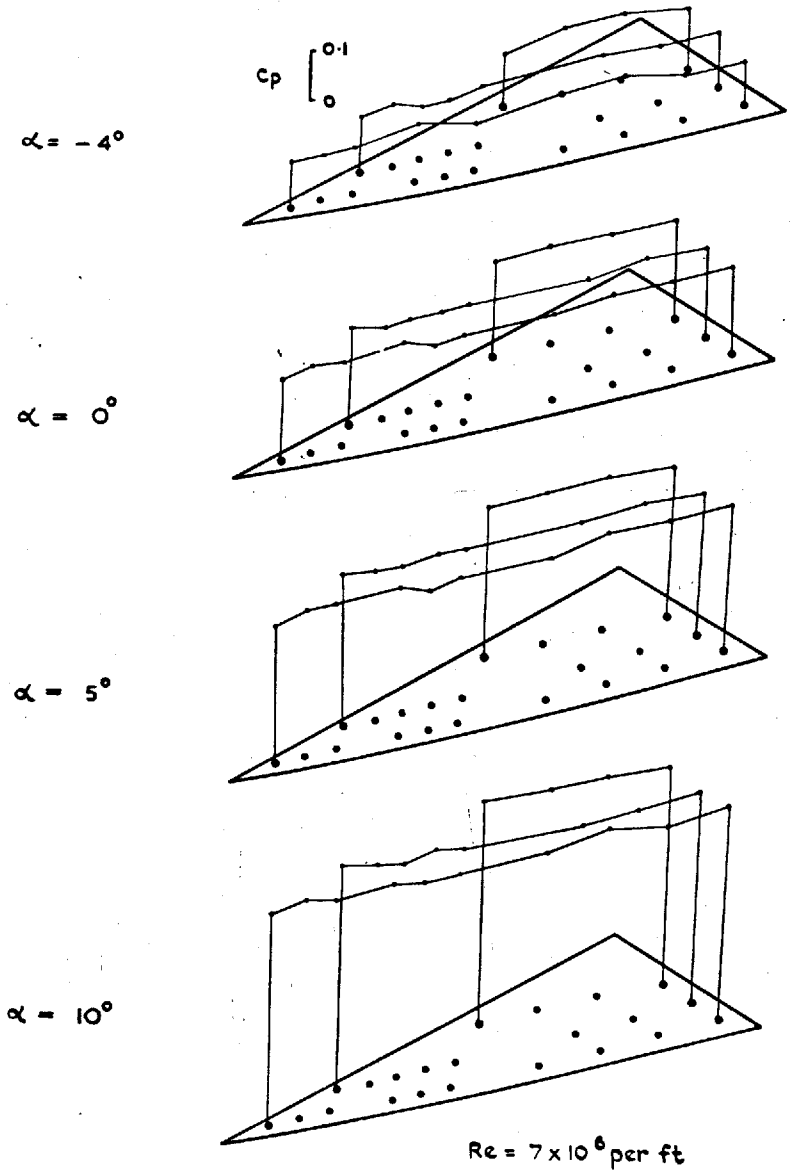


Fig.5b Experimental pressures on a wing from a 16° cone flow at M=4

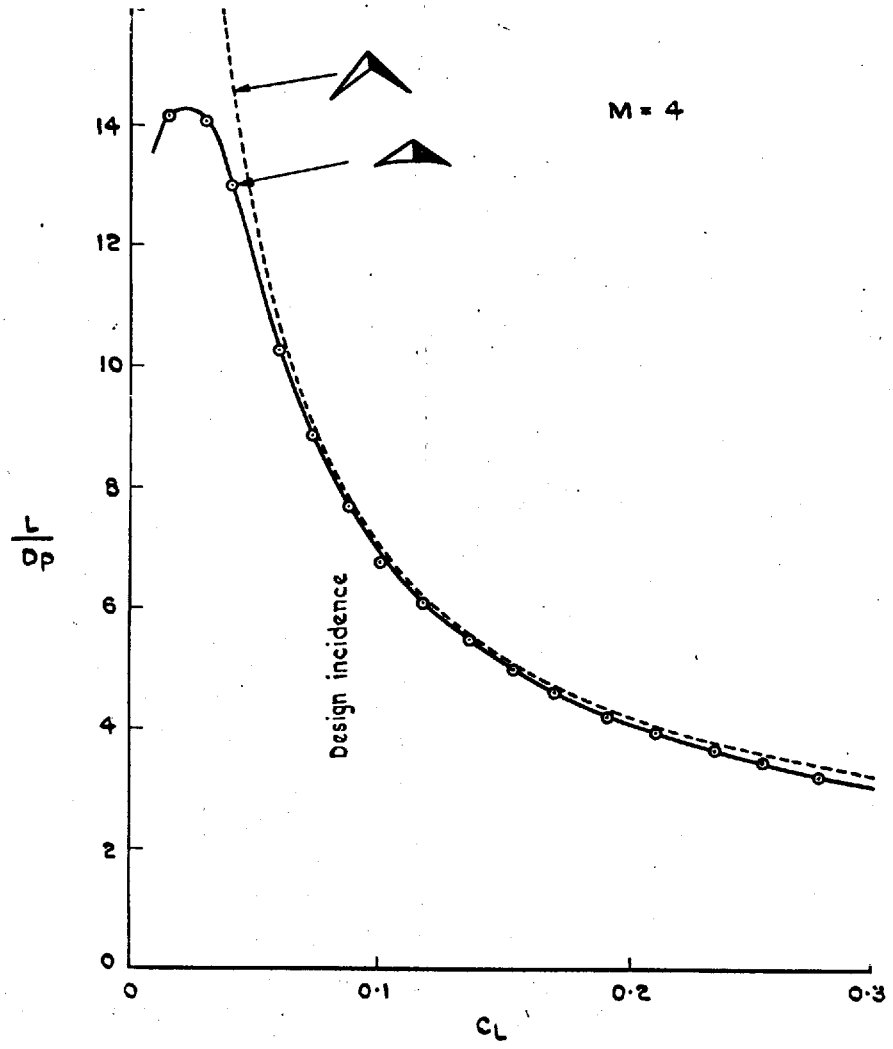


Fig.6 Lift over pressure drag v lift coefficient (11° cone flow model)

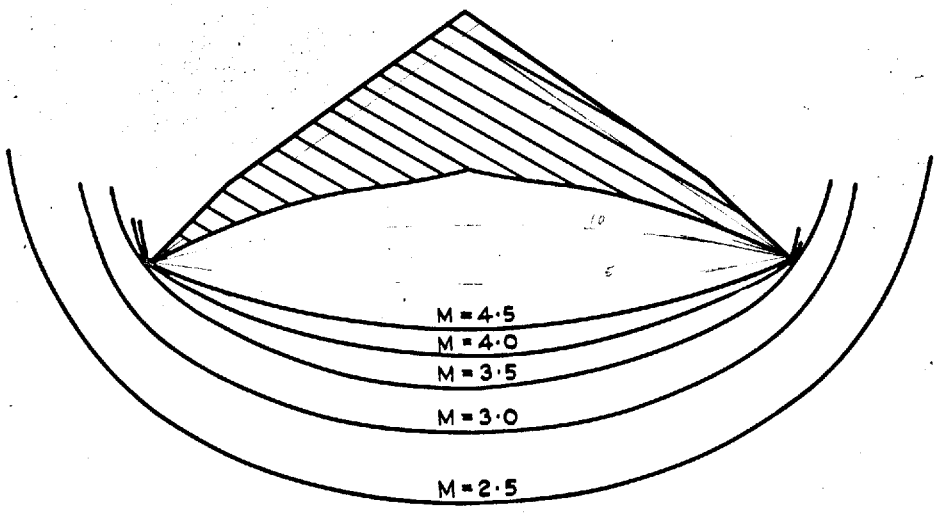


Fig. 7 Shock wave shape at various Mach numbers (11° cone flow model at 0·52 chord)

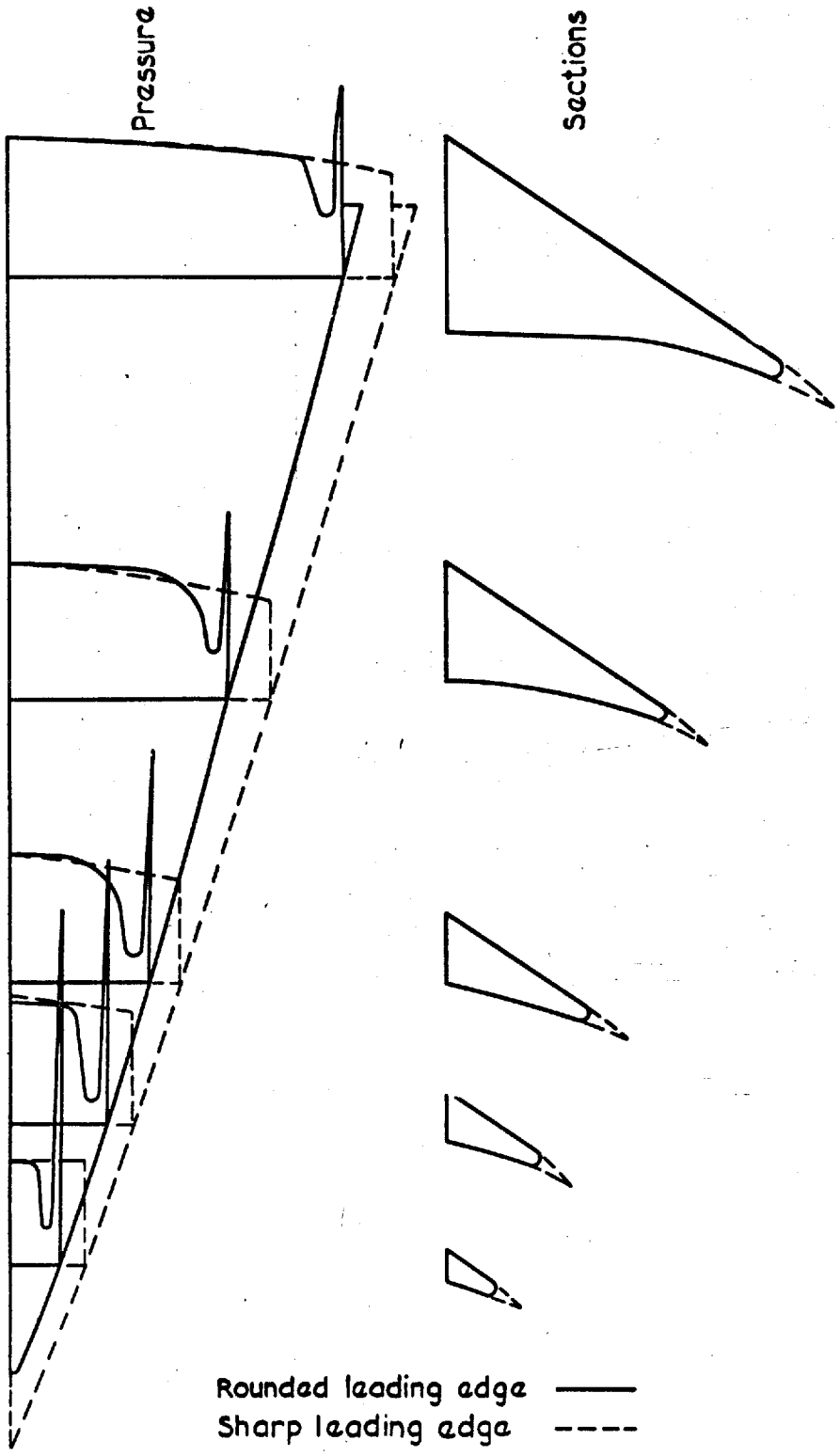


Fig. 8 Comparison of sections and pressures on rounded and sharp leading edge cone flow wings at $M = 4$